4th International Conference on the Durability of Concrete Structures
24–26 July 2014
Purdue University, West Lafayette, IN, USA

Research on Embedded Sensors for Concrete Health Monitoring Based on Ultrasonic Testing

Shifeng Huang, Mimi Li, Yuesheng Xu, Dongyu Xu, Xinchun Xie, and Xin Cheng
Shandong Provincial Key Laboratory of Preparation and Measurement of Building Materials, University of Jinan

ABSTRACT

In this article, embedded ultrasonic sensors were prepared using 1–3-type piezoelectric composite and piezoelectric ceramic as the piezoelectric elements, respectively. The frequency bandwidth of the novel embedded ultrasonic sensors was investigated. To obtain the relationship between the receiving ultrasonic velocity and compressive strength, as well as their response signals to crack damage, the sensors were fabricated and embedded into the cement mortar before testing. The results demonstrated that the piezoelectric composite sensor had wider frequency bandwidth than the piezoelectric ceramic sensor. The compressive strength and ultrasonic velocity had a positive linear relationship, with a correlation coefficient of 0.9216. The head wave amplitude of the receiving ultrasonic signal was sensitive to the changing crack damage and gradually decayed with the increasing degree of cement damage. Thus, the novel embedded ultrasonic sensors are suitable for concrete health monitoring via ultrasonic non-destructive testing.

Keywords: compressive strength, crack, embedded ultrasonic sensor, frequency bandwidth, piezoelectric composite.

1. INTRODUCTION

Concrete is one of the most important structural engineering materials, whose reliability and safety are critically relevant issues in the civil engineering. Thus, these structural components require sophisticated nondestructive techniques to evaluate a range of physical phenomena, particularly the degradation of pre-existing structures and infrastructure (Benedettia, Aliabadib, & Milazzoa, 2010; Purnell, Gan, & Hutchins, 2004). Ultrasonic testing technology has been widely used and numerous studies have attempted to use the ultrasonic velocity (γ_p; in km/s) and its amplitude as measures of compressive strength (S, in MPa) and crack damage for evaluating the performance of concrete; several datasets on the correlation between the S and νp of concrete have been presented (Gregor, Franci, & Goran, 2009; Popovics, 2007).

Ultrasonic sensors are important components of ultrasonic testing technology, which have been discussed in several studies (Chaki & Bourse, 2009; Chih & San, 2012). However, ultrasonic sensors continue to have inherent disadvantages, such as the need for physical contact between the concrete surface and the signal sensors. The concrete surfaces are rarely smooth enough to enable simple contact to provide sufficient acoustic coupling; the performance of a sensor on the concrete surface is easily influenced by the outside environment (Xu, Qin, Huang, & Cheng, 2012). Therefore, embedded ultrasonic sensors with high interface/acoustic impedance matching abilities should be developed for cement materials.

The 1–3-type piezoelectric composite has been widely used as a piezoelectric element in civil engineering health monitoring because of its low acoustic impedance (Z) and mechanical quality factor (Q_m) (Cheng, Xu, Lu, Huang, & Jiang, 2010). Thus, the receiving type embedded ultrasonic sensors were fabricated for this study using the 1–3 polymer-/cement-based piezoelectric composite, whereas the emission type ultrasonic sensor used the piezoelectric ceramic. The relationship between γ_p and S of the cement mortar was investigated using these embedded ultrasonic sensors. The responses of the sensors to crack damage in the cement mortar were simultaneously investigated.

2. EXPERIMENT PROCEDURE

2.1 Raw materials

Sulfate aluminum cement (China United Cement Corporation, China) as well as the lead zirconate titanate PZT-5 and PZT-4 piezoelectric ceramics (Shandong Zibo Yuhai Ceramic Factory, China) were used in this study. Bisphenol A epoxy resin (Shandong Feicheng Deyuan Chemical Co., Ltd., China) and low molecular weight polyamide hardeners (Beijing Xiangshan United Assistant Factory, China) were likewise used. The basic properties of these materials are summarized in Table 1.

Table 1. Main raw materials and their properties.

Material type	tan□/10^{-3}	□r	d_{33}/10^{-12} m V^{-1}	g_{33}/10^{-4} vm n^{-1}	Q_m	K_t	Z/M·Rayl
PZT-5	2	2800	530	22	25	50	24.7
PZT-4	0.3	1050	260	28	1000	0.48	-
Bisphenol A epoxy resin	0.082	2.84	-	-	-	-	-
Cement	0.193	18.9	-	-	-	-	-

2.2 Preparation of the sensor

The PZT-4 piezoelectric ceramic (10 mm × 10 mm × 12 mm) was used as the emission element. The 1–3-type piezoelectric composite was designed of the PZT-5 piezoelectric ceramic to be used as piezoelectric elements of the receiving type ultrasonic sensor. To contrast the properties of the receiving type sensor, a PZT-5 piezoelectric ceramic receiving type sensor was also prepared.

A mixture of cement, epoxy resin, and hardener (cement/polymer) was used as the packaging material for all sensors. To improve the signal-to-noise ratio of the receiving sensor, a piece of shielding wire was retained before packaging. After the solidification of the packaging material, a thin layer of silver paste was used to coat the surface of the sensor before the shielding wire was pasted onto its surface (Figure 1).

Figure 1. The pictures of the receiving sensor.

2.3 Ultrasonic testing

The schematic representation of the cement mortar during ultrasonic testing is presented in Figure 2. The cement mortar was 40 mm × 40 mm ×160 mm in size. An AFG3021B signal generator was used to excite the emission transducer. A TDS1002B digital oscilloscope was used to receive the ultrasonic wave signal. An identical transmitting sensor was excited using one cycle of the 150 kHz square wave with an amplitude of 10 V.

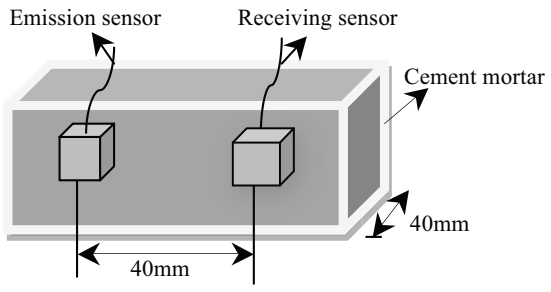

Figure 2. Schematic representation of the cement mortar during ultrasonic testing.

3. RESULTS AND DISCUSSION

3.1 Performance testing of the sensors

Performance testing was conducted in an aqueous environment. The embedded emission and receiving sensors were fixed to the bottom of an organic glass container. The centers of the sensors were kept at the same level, with a 40-mm distance between the two sensors.

The time-domain waveform spectra and the frequency-domain spectra of the receiving ultrasonic waves are shown in Figures 3 and 4, respectively, for the corresponding sensors containing the piezoelectric composite and piezoelectric ceramic. The head wave signals in the time-domain waveform are clearly illustrated in Figure 3, including the specific initial time of the head wave. The receiving signal of the piezoelectric composite sensor had higher amplitude than the piezoelectric ceramic sensor, which is highly significant for judging the propagation velocity of the ultrasonic wave in the cement mortar block.

The piezoelectric composite sensor has larger frequency bandwidth than the piezoelectric ceramic sensor, as shown in Figure 4. The receiving frequency bandwidth of the piezoelectric composite sensor is 126.08 kHz, whereas that of the piezoelectric ceramic sensor is 95.94 kHz. Meanwhile, the piezoelectric composite sensor has the dominant frequency signal.

(1) Velocity–strength relationship

The relationship between the molding time of the cement mortar and the γ_p is shown in Figure 5. The received γ_p significantly increased during the early stages and reached a maximum value after 6 h, before it remained constant. This phenomenon could be attributed to the increased cement hydration reaction time and the subsequent gradual increase in the cement hydration products that mingle together to form the network structure. With the further hardening

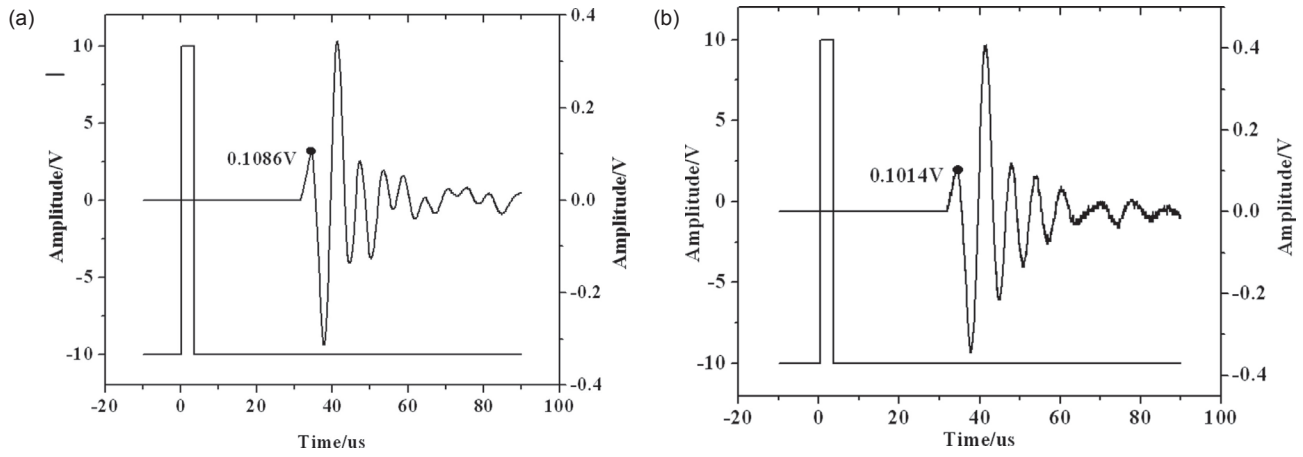

Figure 3. Time-domain waveform spectra of ultrasonic waves received by the embedded sensors. (a) Piezoelectric composite sensor. (b) Piezoelectric ceramic sensor.

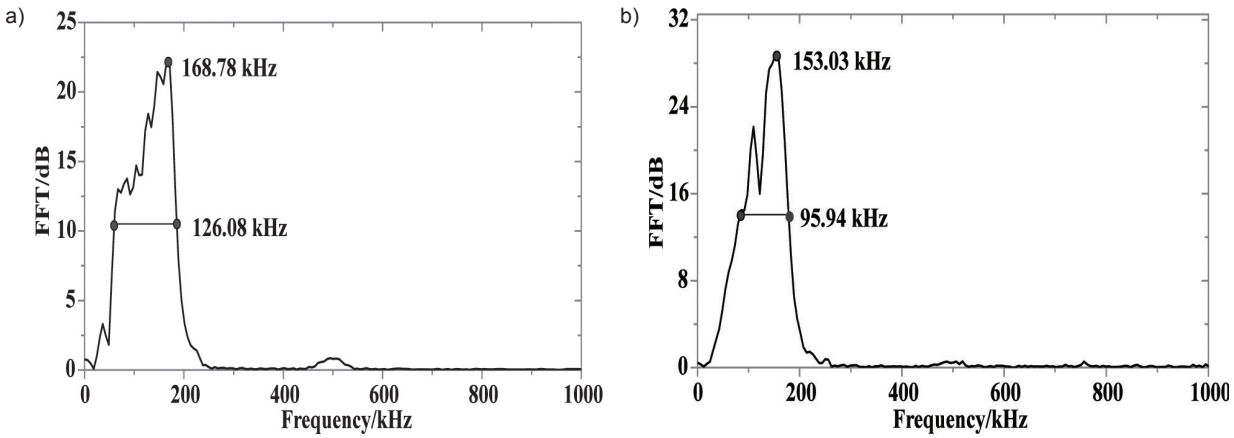

Figure 4. Frequency-domain spectra of ultrasonic waves received by the embedded sensors. (a) Piezoelectric composite sensor. (b) Piezoelectric ceramic sensor.

of the cement paste, the propagation path of the ultrasonic sensor likewise changes from the liquid to solid phase, thereby causing a sharp increase in the received γ_p that eventually stabilizes in the subsequent time points. The received wave velocity of the piezoelectric composite sensor is higher than that of the piezoelectric ceramic sensor.

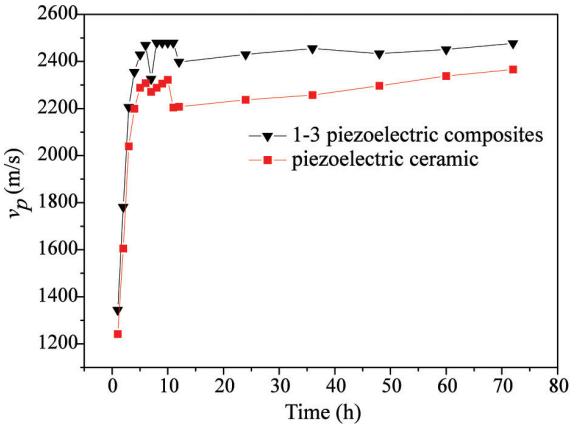

Figure 5. Relationship between molding time and γ_p.

The relationship between the *S* of cement mortar blocks and their γ_p is demonstrated by Figure 6. Positive linear relationships exist between the *S* and γ_p received by the two sensors. As expected, the correlation coefficient of the piezoelectric composite sensor was significantly higher than that of the piezoelectric ceramic sensor. This result is due to the favorable acoustic matching impedance between the piezoelectric composite sensor and the cement mortar. For the media Z_1 and Z_2 with infinite intersection faces, the following reflection coefficient and transmission coefficient are noted when the γ_p propagates from Z_1 to Z_2 along the normal direction:

$$\gamma_p = (z_2 - z_1) / (z_2 + z_1) \quad (3.1)$$

$$\tau_p = 2z_2 / (z_2 + z_1) \quad (3.2)$$

The formula shows that the reflection coefficient decreases with the reduced acoustic impedance difference. Thus, the piezoelectric composite sensor is more suitable for *S* monitoring as compared with the piezoelectric ceramic sensor.

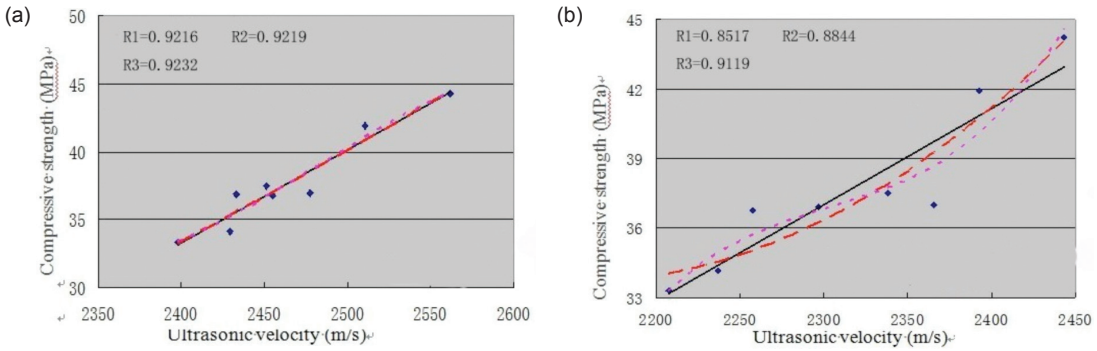

Figure 6. Relationship between γ_p and S. (a) Piezoelectric composite sensor. (b) Piezoelectric ceramic sensor.

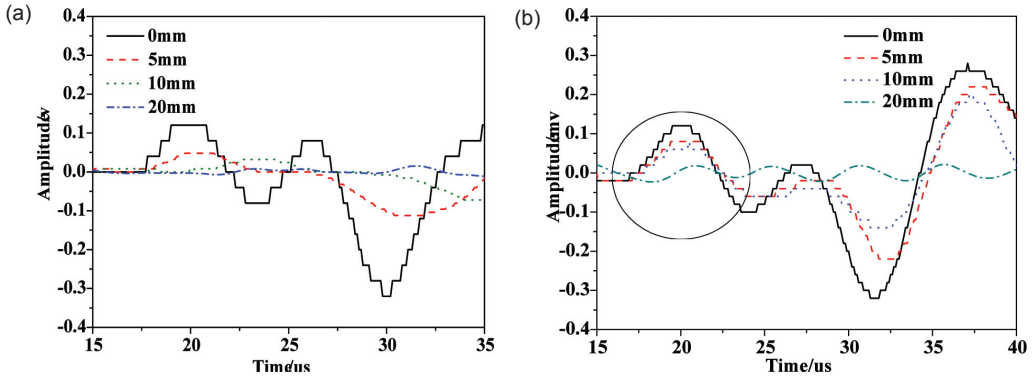

Figure 7. Time-domain waveform spectra of the damaged block. (a) Piezoelectric composite sensor. (b) Piezoelectric ceramic sensor.

(2) Crack damage monitoring

To study the characteristic response of the sensors to crack damage, different crack depths were created in the center of the emission and receiving sensors. The tested depths of the cracks were 0, 5, 10, and 20 mm, respectively.

The ultrasonic signal diagrams of the different crack depths are shown in Figure 7. The head wave amplitude of the ultrasonic signals received by the piezoelectric composite sensor and the piezoelectric ceramic sensor was highly sensitive to crack damage. The signal received by the piezoelectric composite sensor had an obvious head wave. The head wave amplitude decreased with the increasing crack depth, with slightly longer propagation times of the ultrasonic signals. Ultrasonic attenuation is due to the decay rate of elastic mechanical radiation as it propagates through the material. In the one-dimensional case, the linear attenuation coefficient (ξ) can be introduced by considering the decay of a wave traveling in the z direction:

$$u = u_0 e^{-2\xi z} \tag{3.3}$$

where u is the reduced amplitude of the wave after traveling a distance z, whereas u_0 is the amplitude of the wave at the initial location. The presence of damages affects the attenuating behavior of the materials by increasing the energy loss. The increased damage increases the value of ξ, with a consequent decrease of u.

4. CONCLUSION

The embedded ultrasonic sensor that was made using the piezoelectric composite has a wider frequency bandwidth than the piezoelectric ceramic sensor. Its frequency bandwidth had a maximum of 126.08 kHz.

A positive linear relationship exists between the S and the γ_p. The correlation coefficient of the signals received by the piezoelectric composite sensor reached 0.9216.

The head wave amplitude of the receiving ultrasonic signal is sensitive to the changes in the crack damage. This ultrasonic signal has a tendency to decrease with increasing damage.

ACKNOWLEDGMENTS

This work is supported by the National Science Foundation of China (Grant No. 51172097, 51072069) and the Shandong Natural Science Foundation (Grant No. ZR2012EMQ010).

REFERENCES

Benedettia, I., Aliabadib, M. H., & Milazzoa, A. (2010). A fast BEM for the analysis of damaged structures with bonded piezoelectric sensors. *Computational Methods in Applied Mechanical Engineering, 199*, 490–501.

Chaki, S., & Bourse, G. (2009). Guided ultrasonic waves for non-destructive monitoring of the stress levels in presressed steel strands. *Ultrasonics, 42*, 162–171.

Cheng, X., Xu, D. Y., Lu, L. C., Huang, S. F., & Jiang, M. H. (2010). Performance investigation of 1-3 piezoelectric ceramic–cement composite. *Materials Chemistry Physics, 121*, 63–69.

Chih, Y. C., & San, S. H. (2012). Implementing RFIC and sensor technology to measure temperature and humidity inside concrete structures. *Construction and Building Materials, 26*, 628–637.

Gregor, T., Franci, K., & Goran, T. (2009). Prediction of concrete strength using ultrasonic pulse velocity and artificial neural networks. *Ultrasonics, 49*, 53–60.

Popovics, S. (2007). Analysis of the concrete strength versus ultrasonic pulse velocity relationship. *Journal of American Society of Nondestructive Testing*.

Purnell, P., Gan, T. H., & Hutchins, D. A. (2004). Noncontact ultrasonic diagnostics in concrete: A preliminary investigation. *Cement and Concrete Research, 34*, 1185–1188.

Xu, D. Y., Qin, L., Huang, S. F., & Cheng, X. (2012). Fabrication and properties of piezoelectric composites designed for process monitoring of cement hydration reaction. *Materials Chemistry and Physics, 132*, 44–50.